Different glutamate receptors convey feedforward and recurrent processing in macaque V1

Matthew W. Self[a,1], Roxana N. Kooijmans[a], Hans Supèr[b], Victor A. Lamme[c], and Pieter R. Roelfsema[a,d]

[a]Department of Vision and Cognition, Netherlands Institute for Neuroscience (KNAW), 1105 BA, Amsterdam, The Netherlands; [b]Institucio Catalana de Recerca i Estudis Avancats (ICREA) and Departmento de Psicologia Basica, Facultad de Psicologia, Universidad de Barcelona, 08035 Barcelona, Spain; [c]Brain and Cognition, Department of Psychology, University of Amsterdam, 1018XA, Amsterdam, The Netherlands; and [d]Department of Integrative Neurophysiology, Centre for Neurogenomics and Cognitive Research, Vrije Universiteit, 1081HV, Amsterdam, The Netherlands

Edited by Peter H. Schiller, Massachusetts Institute of Technology, Cambridge, MA, and approved April 23, 2012 (received for review November 28, 2011)

Neurons in the primary visual cortex (V1) receive feedforward input from the thalamus, which shapes receptive-field properties. They additionally receive recurrent inputs via horizontal connections within V1 and feedback from higher visual areas that are thought to be important for conscious visual perception. Here, we investigated what roles different glutamate receptors play in conveying feedforward and recurrent inputs in macaque V1. As a measure of recurrent processing, we used figure–ground modulation (FGM), the increased activity of neurons representing figures compared with background, which depends on feedback from higher areas. We found that feedforward-driven activity was strongly reduced by the AMPA receptor antagonist 6-cyano-7-nitroquinoxaline-2,3-dione (CNQX), whereas this drug had no effect on FGM. In contrast, blockers of the NMDA receptor reduced FGM, whereas their effect on visually driven activity varied with the subunit specificity of the drug. The NMDA receptor blocker 2-amino-5-phosphonovalerate (APV) caused a slight reduction of the visual response, whereas ifenprodil, which targets NMDA receptors containing the NMDA receptor NR2B subunit, increased the visual response. These findings demonstrate that glutamate receptors contribute differently to feedforward and recurrent processing in V1 and suggest ways to selectively disrupt recurrent processing so that its role in visual perception can be elucidated.

The areas of the primate visual cortex are arranged in a hierarchy, with feedforward connections propagating information from lower to higher areas and feedback connections carrying information in the opposite direction, back to the lower areas (1). Feedforward and recurrent processing differ greatly in function. Feedforward connections drive neurons in the visual cortex. They shape the receptive field of neurons, causing the rapid formation of tuning properties such as orientation and direction selectivity (2) and even sensitivity to complex objects such as faces. In contrast, recurrent input, carried by feedback connections from higher areas and by horizontal connections within a visual area, is thought not to drive neurons but to mediate modulatory, contextual effects (3, 4). Recurrent connections have been suggested to be involved in attention (5–7), figure–ground segregation (8–11), and conscious visual perception (12, 13), although their precise function is not well understood. One problem in studying the role of recurrent connections has been the lack of a tool to selectively inhibit them without disrupting feedforward processing. Some studies blocked the source of recurrent processing by suppressing activity in higher-level visual areas using cooling or injections of GABA while recording in lower-level areas (9, 14, 15). The results of these studies vary because some showed strong effects on V1 activity (15) and a decrease in contextual modulation (9), whereas others showed no effect (14). The exact effect of recurrent input into V1, therefore, remains to be elucidated.

Why might feedforward connections drive neuronal activity, whereas recurrent connections are merely modulatory? Long-range projections within the visual system use glutamate as an excitatory neurotransmitter (16), and modeling studies (17, 18) have hypothesized that AMPA receptors (AMPA-Rs) carry the feedforward signal from the thalamus to higher visual areas, whereas NMDA receptors (NMDA-Rs) are responsible for the recurrent effects. This would explain why recurrent connections are modulatory because activation of the NMDA-R is dependent on prior depolarization of the postsynaptic neuron (19). If feedback connections use NMDA-Rs, they will have strong effects on neurons that are well driven by AMPA-ergic feedforward input and weaker effects on cells that are not strongly activated, in accordance with the neurophysiology of feedback effects (5, 20, 21). In support of the different roles of these glutamate receptors, the feedforward input from the LGN into visual cortex is sensitive to broad-spectrum glutamate receptor antagonists but much less affected by application of 2-amino-5-phosphonovalerate (APV) (22), a selective NMDA antagonist. Furthermore, a study that activated neurons in cat visual cortex with stimuli of varying contrast found that NMDA-Rs influence response gain; NMDA blockers reduce the response of neurons driven by a high contrast stimulus but have weak effects on responses evoked by low-contrast stimuli and on spontaneous activity (23). In contrast, the effects of AMPA-Rs were additive; AMPA-Rs added to activity in a manner that was relatively independent of contrast. Taken together, these results suggest that AMPA-Rs could drive cortical neurons, whereas NMDA-Rs determine response gain. Here, we aimed to test directly the relative contributions of AMPA-Rs and NMDA-Rs to feedforward input and recurrent processing. We injected antagonists of glutamate receptors into area V1 of two monkeys performing a figure–ground segregation task. We chose this task because the effects of feedforward and recurrent connections are expressed in different phases of the neuronal response (11, 24). The initial response reflects feedforward input from the thalamus and does not discriminate between figure and ground. However, ~100 ms after stimulus onset, V1 neurons increase their firing rate when their receptive field (RF) falls on a figure compared with when it falls on the background (11). This figure–ground modulation (FGM) represents a modulatory influence on the neuronal response from outside the classical RF that correlates well with the percept of the animal (25), and previous studies have pointed to feedback from extrastriate visual areas as the main source of FGM (9, 26, 27). To discriminate between the effects of glutamate receptor classes, we injected 6-cyano-7-nitroquinoxaline-2,3-dione (CNQX) and APV, which are selective antagonists of the AMPA-R and NMDA-R, respectively. There are several subclasses of NMDA-Rs with different NR2 subunits that have distinct functional properties and expression profiles (28). To distinguish the roles that these different receptors play in visual processing, we also injected ifenprodil in some of our experiments, which is a drug

Author contributions: M.W.S., H.S., V.A.L., and P.R.R. designed research; M.W.S. and R.N.K. performed research; M.W.S. analyzed data; R.N.K. suggested the use of ifenprodil and helped perform the ifenprodil recordings; and M.W.S. and P.R.R. wrote the paper.

The authors declare no conflict of interest.

This article is a PNAS Direct Submission.

See Commentary on page 10749.

[1]To whom correspondence should be addressed. E-mail: m.self@nin.knaw.nl.

This article contains supporting information online at www.pnas.org/lookup/suppl/doi:10.1073/pnas.1119527109/-/DCSupplemental.

that selectively blocks NMDA-Rs containing the NR2B subunit (29). We found that CNQX strongly reduced neural firing but that it had little effect on FGM. In contrast, NMDA-R blockers had variable effects on the feedforward response depending on the NMDA-R subunit that they targeted; APV caused a moderate reduction in visually driven activity, but ifenprodil caused a moderate increase. Importantly, despite their opposite effects on the visually driven activity, both drugs reduced FGM.

Results

Task and Behavior. We used a version of the figure–ground segregation task (25) where the monkey was required to indicate the location of a texture-defined figure with a saccade (Fig. 1). On catch trials (25% of trials), the texture was presented with no figure present, and the monkey was required to maintain fixation. The figures were salient because previous reports have demonstrated that these produce strong FGM in V1 (25). The monkeys performed the task with high accuracy. If the figure was present, monkey S was correct on 95.8% and monkey E was correct on 98.0% of the trials. Accuracy on catch trials was somewhat lower (monkey S = 74.5% correct; monkey E = 91.7% correct).

Effect of NMDA-R Antagonists at Example Recording Sites. We recorded the envelope of the multiunit activity (MUAe) simultaneously from the different laminae of V1 in three hemispheres of the two monkeys with a multicontact electrode ("U-probe"; Plexon). In addition to 24 recording sites, the electrode contained a fluid line, which allowed us to pressure-inject small quantities (25–100 nL) of drugs into V1 (Fig. S1). We placed the electrode at the desired depth in cortex using current-source density analysis (Fig. S2) and measured the location and size of the multiunit RFs for each recording site (Fig. S3). We then presented figure–ground textures and ensured that the RF fell either in the center of the figure or in the background region (Fig. 1*B*). We quantified the effect of the drugs using two measures: the peak response and FGM. The peak response was measured as the average activity across both conditions in a window from 50 to 100 ms after stimulus onset. FGM was measured as the difference between the figure and background response from 100 to 200 ms after figure onset expressed as a fraction of the peak response. All MUAe responses before and after drug application were normalized to the peak response of the predrug epoch for each recording site. An example recording in which we injected APV is illustrated in Fig. 2*A*. In the predrug control period, we observed the typical FGM profile. After ~100 ms, the response evoked by the figure (thick, dark blue trace) became stronger than activity evoked by the homogeneous background (thin, light blue trace). After this baseline measurement, we injected 30 nL of 50 mM APV. The example in Fig. 2*A* shows the typical effect of APV. The drug caused a small reduction in peak response by 9% of the predrug level ($P < 0.01$; *t* test). In the later response phase, APV reduced the figure response, but it barely affected the background response. This led to a reduction in FGM, by 46.2% of the predrug level (ANOVA; $F_{1,463} = 5.6$, $P < 0.02$). To investigate whether the decrease in FGM was caused by the change in response strength, we calculated a modulation index (MI), which is insensitive to the overall level of activity because it is defined as the difference between the figure and ground response in a window from 100 to 200 ms after stimulus onset divided by the summed activity in that window [MI = (figure − ground)/(figure + ground)]. APV reduced the MI from 0.13 to 0.07 (a 41.8% reduction), which indicates that the reduction in FGM was larger than the reduction in overall activity. In a few penetrations, the visual response increased after APV application, but FGM was reduced (Fig. S4). FGM recovered well within 60 min of drug application. We also studied injections of ifenprodil, which is an NMDA antagonist that predominantly inactivates NMDA-Rs containing the NR2B subunit. Fig. 2*B* shows a recording site where we injected ifenprodil, which to our surprise caused an increase in the peak response by 11.5% ($P < 0.01$; *t* test), an effect that was typical for ifenprodil injections. Despite this increase in activity, we found that ifenprodil reduced the level of FGM, in this example by 94% of the predrug level (ANOVA; $F_{1,450} = 4.73$; $P = 0.03$). The combination of an increase in overall activity with a decrease in FGM reduced the MI from 0.14 to 0.005 (a 96% reduction). We did not observe much recovery from the ifenprodil injection, even though we waited for over 1.5 h after the injection, but this result is not unexpected because long recovery times have also been reported for ifenprodil in cortical slices (30) (Fig. S5).

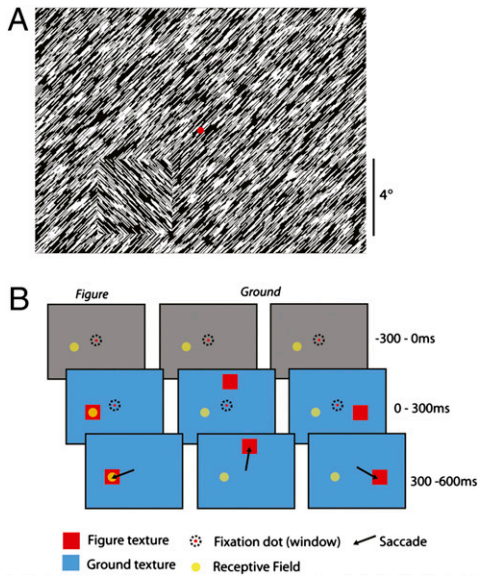

Fig. 1. Behavioral task and recording method. (*A*) Example of a figure–ground texture with a figure composed of 135°-oriented lines on a background of lines oriented at 45°. The red circle in the center of the display is the fixation point. (*B*) Schematic representation of the main conditions with the multiunit RF inside or outside the figure. In the ground condition, the figure was placed at one of two possible locations at an angle of 120° from the RF position, at the same eccentricity. The task of the monkey was to make a saccade into a target window centered on the figure, after the fixation point was extinguished.

Effects of NMDA-R Antagonists at the Population Level. Across the population of recording sites, we observed that APV ($n = 388$) and ifenprodil ($n = 295$) had opposite effects on the visually driven response. APV decreased visual responses by an average of 7.5% if we analyzed the entire response epoch (0–200 ms) (Fig. 3*A*). APV reduced both the peak response (50–100 ms) by 8.3% (Fig. 3*B*; *t* test; $P < 0.05$ in both monkeys) and the later sustained response (100–200 ms) by 8.1% (*t* test; both $P < 0.001$; Fig. 3*C*). In contrast, ifenprodil reliably increased neural responses (Fig. 3*A*). Across the population of recording sites, the average increase in peak response was 7.8%, and responsiveness also increased in the later analysis window (*t* tests; all *P* values, <0.001 for both monkeys) (green symbols in Fig. 3 *B* and *C*). Despite their opposite effects on visual responsiveness, both NMDA antagonists reduced FGM. APV reduced responses in both the figure and ground conditions, but the reduction was greater in the figure condition leading to the decrease in FGM (Fig. 3*C*). APV reduced FGM by 34.2% across all penetrations (Fig. 4*A*; *t* test; both monkeys, $P < 0.001$). Moreover, this decrease in FGM was stronger than predicted by the decrease in visual responsiveness, so that the MI was also reduced, from 0.14 to 0.10 (22.2% reduction; *t* test; both monkeys $P < 0.05$; Fig. 4*B*). Fig. 4*C* shows the effect of APV across individual penetrations. The majority of penetrations exhibited significant reductions in FGM. In some, FGM was not reduced, but we could not exclude that the injection failed in some of these experiments. Ifenprodil

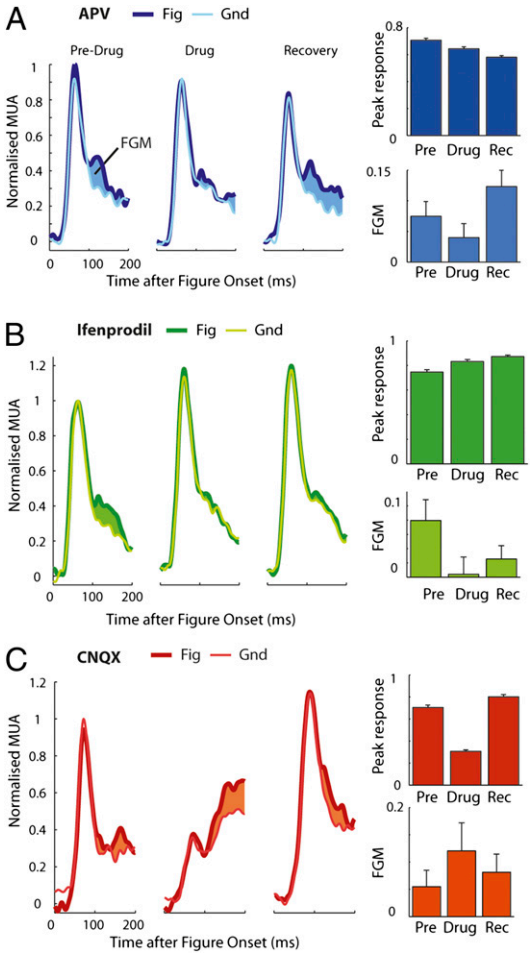

Fig. 2. Example drug effects on neuronal activity in area V1. (*A*) Multiunit neuronal responses at an electrode situated in the superficial layers before and after the injection of 40 nL of APV. Thick and thin traces show MUAe responses evoked by the figure and background, respectively, and the shaded regions indicate the FGM. The data shown here were normalized by the maximum response across conditions in the predrug period. The data from the recovery period were obtained 1 h after the injection. The bar graphs on the right show the effect of the drug on the peak response, which was defined as the average activity evoked by figure and background from 50 to 100 ms after stimulus onset (upper graph) and on FGM, which was defined as the difference between the response evoked by figure and background in a window from 100 to 200 ms after stimulus onset. The error bars show the SEM. (*B*) Effects of a 30-nL injection of ifenprodil at a layer 4 electrode that caused an increase in peak response and a decrease in FGM that did not recover, although the session was continued for 1.5 h postinjection. (*C*) Example of a 30-nL injection of CNQX that produced a decrease in the peak response but did not reduce FGM; the electrode was situated in the superficial layers. The data from the recovery epoch were recorded more than 90 min after the injection.

also reduced FGM. It increased responses evoked by the figure and by the background, but the increase was greater for the background responses, causing a decrease in FGM (Fig. 3*C*). Ifenprodil caused significant reductions in FGM in 10 out of 17 penetrations (Fig. 4*D*). Across all recording sites, the average reduction in FGM was 21.5% (*t* test; both monkeys, $P < 0.001$; Fig. 4*A*). Moreover, this reduction in FGM combined with an increase in visually driven activity reduced the MI from an average value of 0.19 to 0.13 (33.2% reduction; *t* test; both monkeys, $P < 0.001$; Fig. 4*B*). The time course of the effect of the two drugs differed. APV produced immediate effects, which recovered well within 30 min (yellow bars in Fig. 4 *A* and *B*), whereas the effects of ifenprodil took longer to reach their maximum and were relatively long-lasting, so that the changes in neuronal activity did not return to baseline, even if the recording session was extended to >2 h postinjection (30) (Fig. S5). The effects of the two drugs also differed across the different layers of V1 (Fig. S6). Responses during catch trials were very similar to responses during the ground condition (triangles in Fig. 3 *B* and *C*), although responses from monkey E were slightly, but significantly (*t* test; $P < 0.001$), higher during catch trials than ground trials. This difference indicates that the presence of a figure elsewhere caused a decrease in the response evoked by the background. The drugs did not influence this difference between catch and ground trials (*t* test, $P > 0.05$).

Effects of an AMPA-R Antagonist. In separate experiments, we injected CNQX, which is an antagonist of the AMPA-R. Fig. 2*C* shows an example recording site where CNQX was injected. In this example, CNQX produced a large reduction in the peak response by 56.5% of the predrug level ($P < 0.001$; *t* test). Interestingly, the decrease in peak response was not accompanied by a significant change in FGM (ANOVA; $F_{1,785} = 1.19$; $P = 0.28$). In this example, responses recovered within 90 min of the injection. The effects of CNQX on the overall response level were consistent across the population with 93.5% of recording sites ($n = 252$) showing a reduction in response (Fig. 3 *A* and *B* and Fig. S7*A*). The drug reduced the initial peak response on average by 37.5% of the predrug level (*t* test; both monkeys, $P < 0.001$; Fig. 3 *A* and *B*). At the population level, the decrease in activity during the later sustained response phase was similar to the reduction in peak response (reduction of 26.1%;*t* test; both monkeys, $P < 0.01$; Fig. 3*C*). The effects of CNQX on the figure and background responses were similar (Fig. 3*C*), and the drug, therefore, did not cause a significant reduction in either FGM (*t* test; $P = 0.17$) or MI (*t* test; $P = 0.27$) (Fig. 4 *A* and *B* and Fig. S7*C*). Recovery from CNQX injections was partial, and its effect on the visually driven response recovered by ~85% (yellow bar in Fig. 3*A*). As a control for the effects of the pressure injection, we also carried out separate penetrations in which we injected water or artificial cerebrospinal fluid (aCSF) for a total of 224 recording sites. These control injections had no effect on the peak response (*t* test; $P > 0.05$) (black symbols in Figs. 3 and 4; also see Fig. S7 *B* and *D*), FGM (*t* test; $P > 0.05$), or MI (*t* test; $P > 0.05$). Control analyses demonstrated that the effects reported here could not be explained by small changes in fixational eye movements (*SI Results*).

Discussion

Here, we have investigated the involvement of different glutamate receptors in the various processing phases of a texture segregation task. We chose this task because neuronal responses in area V1 can be separated into two phases: (*i*) an initial peak response (50–100 ms) in which neural responses do not distinguish between figure and ground; and (*ii*) a later sustained period of firing (100 ms and onward) in which the figure–ground context modulates the V1 activity. Because our main analyses relied on MUA recording (see *Materials and Methods* and Fig. S8 for details), we considered the possibility that these response phases are carried by different cells, which are mixed in the MUA. However, previous studies reported that virtually all V1 neurons first exhibit a transient response in the texture-segregation task, followed by a weaker sustained firing rate (see Fig. S9*A* for an example) that is modulated by figure–ground segregation for a sizable fraction of the cells (8, 11). Thus, the transient response and the figure–ground modulation are evoked in the same neurons. The initial peak response provides a measure for the feedforward input and the rapid local analysis that takes place within V1. We found that the initial visual response was very sensitive to CNQX, indicating a strong contribution of AMPA-Rs, in accordance with previous studies (22, 31, 32). The extent to which NMDA-Rs contribute to the visually driven response is a matter of debate, because some studies reported that APV suppresses visual responses (31, 33), whereas other studies found that NMDA-Rs do not contribute strongly to visually driven

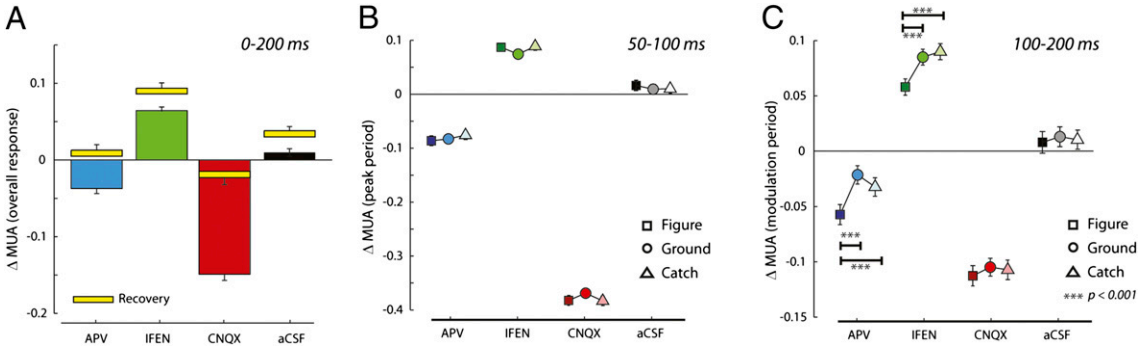

Fig. 3. Drug effects on visual responsivity across recording sites. (*A*) Average change in overall response (from 0 to 200 ms after stimulus onset, averaged across figure and ground conditions) across all recording sites after injections of APV (blue), ifenprodil (green), CNQX (red), and aCSF (black). The graph shows the change in response compared with the predrug baseline. (Negative numbers indicate a decrease in response.) Yellow bars indicate the response in the recovery epoch. Error bars denote SEM across recording sites. (*B*) Effect of the different drugs on the activity during the peak response window (50–100 ms after stimulus onset) for the figure (squares), ground (circles), and catch trials (triangles). The predrug activity has been subtracted, and negative values, therefore, indicate that the drug reduced the response. The effects of the drugs on the responses evoked by the figure and background were identical in this time window. (*C*) Change in response during the modulation period (100–200 ms after stimulus onset). The difference between the effect of the drugs on activity evoked by the figure and ground corresponds to the drug effect on FGM (reported in Fig. 4*A*). ***$P < 0.001$ (paired *t* test).

activity in layer 4 or 6 (22, 23, 34). We found that antagonists of the NMDA-R affected the visually driven activity but that the effect depended on the subunit specificity of the antagonist. Injections of APV, which blocks all NMDA-R subtypes, generally reduced neural activity. A remarkable finding is that ifenprodil, which preferentially blocks NMDA-Rs containing the NR2B subunit, consistently increased neural activity. One possibility is that these receptors promote inhibition of V1 activity, so that blocking them disinhibits cortical columns.

During the later, sustained response phase, V1 neurons fire more strongly if their RF falls on a figure than on a background region. This FGM is thought to arise from feedback from higher visual areas (9, 26, 27, 35) with possible contributions from horizontal connections within area V1 (36). The relative contribution of these potential sources of FGM is not known, and it is, therefore, convenient to refer to these modulatory effects as "recurrent." Our results show that blocking AMPA-Rs causes a robust suppression of visually driven activity without much effect on FGM. In contrast, FGM was sensitive to drugs that block the NMDA-R because both APV and ifenprodil significantly reduced FGM despite their opposite effects on the visually driven activity. This dissociation between the effects of drugs targeting the AMPA and NMDA-Rs suggests that feedforward information is predominantly carried by AMPA-Rs, whereas FGM depends on NMDA-Rs. APV and ifenprodil also differed in the manner by which they reduced FGM. APV produced a greater suppression of responses evoked by figures compared with the background, whereas ifenprodil produced a greater increase of background responses than of figure responses. This latter finding raises the intriguing possibility that recurrent connections suppress the response to the background through NMDA-Rs containing the NR2B subunit. Although this hypothesis may seem to be at odds with anatomical studies in the rat visual cortex showing that feedback connections almost exclusively target excitatory neurons (37), comparable studies in the macaque visual cortex are lacking, so that the neuronal targets of feedback projections in primates remain unknown.

Are Feedforward Connections AMPA-Ergic and Recurrent Connections NMDA-Ergic? Theoretical studies have suggested that feedforward connections drive the neurons in a cortical column, whereas recurrent connections can only modulate the activity (3, 4). It is advantageous that recurrent connections do not drive their target neurons, because this could lead to positive-feedback loops causing uncontrolled activity (3). Models of cortical processing suggested that the properties of driving and modulatory connections could be related to differences in the proportion of AMPA-Rs and NMDA-Rs (38). Specifically, AMPA-Rs were suggested to propagate visual activity from lower to higher areas, whereas NMDA-Rs were proposed to cause modulatory effects mediated by recurrent connections (17, 18). On the one hand, AMPA-Rs directly depolarize the postsynaptic neuron, and this could explain the efficient activation of neurons by feedforward connections, which drive cells and determine their tuning (22, 32, 34). The presence of NMDA-Rs in recurrent connections, on the other hand, could explain why these connections are merely modulatory. If gluta-

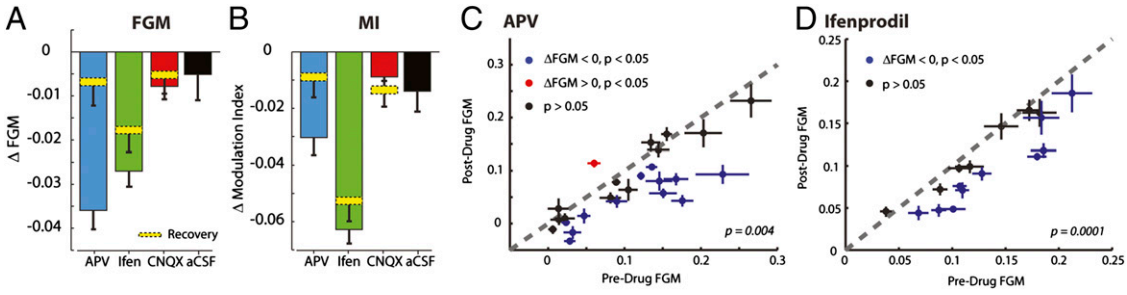

Fig. 4. Drug effects on figure–ground modulation. (*A*) Average change in FGM (in a window from 100 to 200 ms after stimulus onset) across all recording sites after injections of APV (blue), ifenprodil (green), CNQX (red), and aCSF (black). Negative numbers indicate a decrease in FGM. Yellow bars indicate FGM in the recovery epoch, and error bars denote SEM across recording sites. (*B*) Change in MI caused by the drugs. (*C*) Effects of APV on FGM per penetration. *x* axis, average predrug FGM across recording sites of one penetration; *y* axis, postdrug FGM. Error bars show SEM. Penetrations with a nonsignificant effect may have been the result of failed injections. (*D*) Effect of ifenprodil across penetrations.

mate binds to NMDA-Rs, then the channels only pass current upon removal of the magnesium block by sufficient depolarization caused by concomitant activation of AMPA-Rs (19). NMDA-ergic recurrent connections could, thereby, amplify a selective subset of the neuronal responses evoked by AMPA-ergic feedforward connections, and this mechanism could explain why modulatory effects are most pronounced for neurons that are well driven by a visual stimulus (5, 20, 21). NMDA channels of neurons that are not driven by feedforward connections would remain blocked, so that recurrent connections would have little impact on these cells. The idea that feedforward connections use AMPA-Rs and recurrent connections NMDA-Rs is presumably only a first approximation, however, because cortical synapses in adult animals usually contain functional AMPA-Rs as well as NMDA-Rs (39). Nevertheless, there are substantial differences in the AMPA/NMDA ratio between cortical areas and also between layers within area V1 (34, 40–42), which suggest that recurrent connections may target synapses that are richer in NMDA-Rs than feedforward connections. A previous study in anesthetized cats (23) supported the different roles of these glutamate receptors by showing that activation of AMPA-Rs added a relatively constant number of spikes to the firing rate of a neuron, whereas activation of the NMDA-R caused an increase in response gain. Similarly, a study on direction selectivity (43) showed that AMPA-R activity produces directionally selective responses, whereas NMDA-R activity amplifies neuronal responses evoked by a stimulus moving in the preferred direction. In other words, NMDA-Rs increase the firing rate of active cells and have little effect on neurons not driven by the visual stimulus.

Other Mechanisms That Could Explain the Effect of NMDA Blockers on FGM. We also considered other explanations for the effects of NMDA antagonists on FGM that do not depend on differences in glutamate receptor distributions. First, we considered the possibility that the differential effect of AMPA and NMDA blockers could be caused by NMDA channels opening more slowly than AMPA channels (19). However, we observed that the NMDA-R antagonists had significant, albeit opposite, effects on the initial transient response, which is incompatible with explanations solely based on differences in receptor dynamics. Second, an intriguing recent study (44) has opened up the possibility that NMDA-Rs play a crucial role in integrating synaptic inputs contacting the apical dendrites of pyramidal neurons, which are key targets for feedback projections (45). The activation of NMDA-Rs induces NMDA spikes, which are regenerative events in the dendritic tufts of cortical neurons that can give rise to a calcium spike. This calcium spike, in turn, propagates along the apical dendrite to the soma to influence the firing rate of the neuron. Blocking of NMDA-Rs reduces the ability of layer I synapses to generate a dendritic calcium spike (44). In our experiment the NMDA blockers may also have prevented the NMDA spikes induced by feedback connections that contribute to figure–ground segregation, leading to a reduction in FGM. We did not completely remove FGM with injections of APV or ifenprodil. It is, therefore, possible that other receptors also contribute to FGM. A recent study that used drugs that target acetylcholine receptors, for example, demonstrated that attentional feedback effects in area V1 depend on the activation of muscarinic receptors (46). However, it is also possible that the partial removal of FGM reflects the small amount of drug that we injected. Higher concentrations and larger quantities might lead to more complete blocks.

Is Feedback to V1 Necessary to Solve the Figure-Ground Task? FGM correlates with the ability of monkeys to segment the image and detect the figure (25). Moreover, FGM does not occur in anesthetized animals (47). These findings suggest that recurrent interactions between area V1 and higher visual areas are necessary to solve the figure–ground segregation task. A strict test of this hypothesis would be to block or reduce FGM in area V1 while allowing the normal feedforward propagation of the visual response. In this study, we observed that NMDA-R antagonists come close to fulfilling these criteria. Both APV and ifenprodil reduce the level of FGM, and the effects of these drugs on the feedforward response are small compared with the effects of CNQX. Our behavioral paradigm was designed to produce strong FGM, and the figures were always well above the threshold for perception. Future studies could use more sensitive behavioral paradigms to test whether the reductions in FGM caused by NMDA blockers interfere with figure perception.

Materials and Methods

Task and Training. All procedures were approved by the Institutional Animal Care and Use Committee of the Royal Netherlands Academy of Arts and Sciences. We recorded from two adult macaque monkeys (*Macaca Mulatta*: monkeys S and E). The monkeys were implanted with a head post for head stabilization and a recording chamber over V1 using standard techniques (*SI Materials and Methods*). The animals were trained to fixate within a window of 1° diameter centered on a small red circular fixation point (0.3° in diameter). We recorded eye movements using a video eye tracker (Thomas Recording) sampled at 250 Hz. Every trial began with the fixation point presented on the gray background, and the monkeys triggered the beginning of the trial when their gaze entered a 1° fixation window centered on the fixation point. After 300 ms of fixation, a full-screen texture stimulus was presented. The texture consisted of black oriented lines (either 45° or 135°) on a white background (Fig. 1*A*). The texture was designed so that, on average, the image elements in the RF were constant across conditions (*SI Materials and Methods*). On figure and ground trials, the texture contained a 4° wide square figure. The location of the figure was varied so that the RFs of the neurons fell on the figure or on the background (Fig. 1*B*). After a further 300 ms, the fixation point was extinguished, and the monkey was required to make a saccade into a target window centered on the figure position. On 25% of trials, we presented a homogeneous texture without a figure (catch condition), and the animals were rewarded for carrying on fixating within the fixation window for a further 400 ms. The stimulus conditions were presented in a pseudorandom order. We made the recordings in epochs of 200 correct trials with each session consisting of at least one predrug epoch, one drug epoch, and one recovery epoch, although we typically recorded several recovery epochs.

Electrophysiological Methods. We used laminar electrodes ("U-probes"; Plexon) for all recordings. We used a 24-contact version of the probe, with a diameter of 420 μm, a contact diameter of 25 μm, and an intercontact spacing of 100 μm. The impedance of the contact points was in the range of 300–700 kΩ at 1 kHz, allowing us to record multiunit data. The recordings were grounded and referenced to the guide tube used to stabilize the transition of the electrode across the dura. (The guide tube did not penetrate the dura.) The head stage amplified the signal by four times before the signal was passed to a preamplifier (Tucker-Davis Technologies). The signal was digitized at 24.4 kHz. As in previous studies (48, 49), we measured the MUAe (*SI Materials and Methods*). The signal was bandpass-filtered (500–5,000 Hz), full-wave-rectified, and then low-pass-filtered (200 Hz) and sampled at a rate of 763 Hz. The MUAe represents the pooled activity of a number of single units in the vicinity of the tip of the electrode, and the population response obtained with this method is, therefore, expected to be identical to the population response obtained by pooling across single units (49). Multiunit RFs were plotted using a moving bar stimulus as reported previously (49) (Fig. S3). Further details about the MUAe recording technique and comparisons with thresholded MUA are provided in *SI Materials and Methods* and Figs. S8–S10.

Data Analysis. The MUAe traces for each trial were filtered with notch filters at 50 and 85 Hz to remove possible contamination from line noise and the monitor refresh rate. For each recording site, we calculated an average response after subtracting the pretrial baseline and then normalizing to the average response in the peak window (50–100 ms) from the predrug, catch-trial condition. The MUAe data we report are, therefore, expressed as fractions of the average peak response, e.g., a change of 0.1 units equals a change of 10% of the peak response. We removed recording sites with a signal-to-noise ratio (SNR) of less than 1 (12.8% of sites). SNR was calculated as the ratio between the peak response and the SD of the spontaneous activity level across trials. For statistical comparisons at the population level, we used two-sided *t* tests for every drug to test whether it changed the visual response or FGM. Because we performed four tests for each time window (three drugs plus control), we applied a Bonferroni correction for multiple comparisons. Results are only reported as significant if the corrected *P* value was less than 0.05 for both monkeys individually

and when averaged across monkeys. The MI [(figure − ground)/(figure + ground)] is an unstable measure for recording sites in which the denominator is close to zero (i.e., sites where the overall response level during the sustained period drops back to baseline). To avoid the average MI across recording sites becoming dominated by extreme values, we removed recording sites in which the sustained period activity was lower than 5% of the peak response or the absolute *z* score of sustained period activity was greater than 3 (3.9% of sites).

ACKNOWLEDGMENTS. We thank Kor Brandsma for help with surgical procedures and animal training and Istvan Ulbert for technical help with the injectrodes. This work was supported by a Netherlands Organization for Scientific Research (NWO)-VICI grant, a grant from the European Union (EU): Information Society Technologies (IST) Cognitive Systems, Project 027198 "Decisions in Motion"), a Human Frontier Science Program (HFSP) grant (to P.R.R.), an NWO-VIDI grant (to H.S.), and an Advanced Investigator grant from the European Research Council (to V.A.L.).

1. Felleman DJ, Van Essen DC (1991) Distributed hierarchical processing in the primate cerebral cortex. *Cereb Cortex* 1:1–47.
2. Hubel DH, Wiesel TN (1968) Receptive fields and functional architecture of monkey striate cortex. *J Physiol* 195:215–243.
3. Crick F, Koch C (1998) Constraints on cortical and thalamic projections: The no-strong-loops hypothesis. *Nature* 391:245–250.
4. Sherman SM, Guillery RW (1998) On the actions that one nerve cell can have on another: Distinguishing "drivers" from "modulators". *Proc Natl Acad Sci USA* 95: 7121–7126.
5. Moore T, Armstrong KM (2003) Selective gating of visual signals by microstimulation of frontal cortex. *Nature* 421:370–373.
6. Roelfsema PR (2006) Cortical algorithms for perceptual grouping. *Annu Rev Neurosci* 29:203–227.
7. Desimone R, Duncan J (1995) Neural mechanisms of selective visual attention. *Annu Rev Neurosci* 18:193–222.
8. Zipser K, Lamme VA, Schiller PH (1996) Contextual modulation in primary visual cortex. *J Neurosci* 16:7376–7389.
9. Hupé JM, et al. (1998) Cortical feedback improves discrimination between figure and background by V1, V2 and V3 neurons. *Nature* 394:784–787.
10. Angelucci A, et al. (2002) Circuits for local and global signal integration in primary visual cortex. *J Neurosci* 22:8633–8646.
11. Lamme VA (1995) The neurophysiology of figure-ground segregation in primary visual cortex. *J Neurosci* 15:1605–1615.
12. Lamme VA, Roelfsema PR (2000) The distinct modes of vision offered by feedforward and recurrent processing. *Trends Neurosci* 23:571–579.
13. Lamme VA (2006) Towards a true neural stance on consciousness. *Trends Cogn Sci* 10: 494–501.
14. Hupé JM, James AC, Girard P, Bullier J (2001) Response modulations by static texture surround in area V1 of the macaque monkey do not depend on feedback connections from V2. *J Neurophysiol* 85:146–163.
15. Sandell JH, Schiller PH (1982) Effect of cooling area 18 on striate cortex cells in the squirrel monkey. *J Neurophysiol* 48:38–48.
16. Johnson RR, Burkhalter A (1994) Evidence for excitatory amino acid neurotransmitters in forward and feedback corticocortical pathways within rat visual cortex. *Eur J Neurosci* 6:272–286.
17. Dehaene S, Sergent C, Changeux JP (2003) A neuronal network model linking subjective reports and objective physiological data during conscious perception. *Proc Natl Acad Sci USA* 100:8520–8525.
18. Lumer ED, Edelman GM, Tononi G (1997) Neural dynamics in a model of the thalamocortical system. I. Layers, loops and the emergence of fast synchronous rhythms. *Cereb Cortex* 7:207–227.
19. Daw NW, Stein PS, Fox K (1993) The role of NMDA receptors in information processing. *Annu Rev Neurosci* 16:207–222.
20. Treue S, Martínez Trujillo JC (1999) Feature-based attention influences motion processing gain in macaque visual cortex. *Nature* 399:575–579.
21. Ekstrom LB, Roelfsema PR, Arsenault JT, Bonmassar G, Vanduffel W (2008) Bottom-up dependent gating of frontal signals in early visual cortex. *Science* 321:414–417.
22. Hagihara K, Tsumoto T, Sato H, Hata Y (1988) Actions of excitatory amino acid antagonists on geniculo-cortical transmission in the cat's visual cortex. *Exp Brain Res* 69: 407–416.
23. Fox K, Sato H, Daw N (1990) The effect of varying stimulus intensity on NMDA-receptor activity in cat visual cortex. *J Neurophysiol* 64:1413–1428.
24. Roelfsema PR, Tolboom M, Khayat PS (2007) Different processing phases for features, figures, and selective attention in the primary visual cortex. *Neuron* 56:785–792.
25. Supèr H, Spekreijse H, Lamme VA (2001) Two distinct modes of sensory processing observed in monkey primary visual cortex (V1). *Nat Neurosci* 4:304–310.
26. Lamme VA, Supèr H, Spekreijse H (1998) Feedforward, horizontal, and feedback processing in the visual cortex. *Curr Opin Neurobiol* 8:529–535.
27. Angelucci A, Bullier J (2003) Reaching beyond the classical receptive field of V1 neurons: Horizontal or feedback axons? *J Physiol Paris* 97:141–154.
28. Köhr G (2006) NMDA receptor function: Subunit composition versus spatial distribution. *Cell Tissue Res* 326:439–446.
29. Williams K (1993) Ifenprodil discriminates subtypes of the N-methyl-D-aspartate receptor: Selectivity and mechanisms at recombinant heteromeric receptors. *Mol Pharmacol* 44:851–859.
30. Kumar SS, Huguenard JR (2003) Pathway-specific differences in subunit composition of synaptic NMDA receptors on pyramidal neurons in neocortex. *J Neurosci* 23: 10074–10083.
31. Sato H, Hata Y, Tsumoto T (1999) Effects of blocking non-N-methyl-D-aspartate receptors on visual responses of neurons in the cat visual cortex. *Neuroscience* 94: 697–703.
32. Armstrong-James M, Welker E, Callahan CA (1993) The contribution of NMDA and non-NMDA receptors to fast and slow transmission of sensory information in the rat SI barrel cortex. *J Neurosci* 13:2149–2160.
33. Miller KD, Chapman B, Stryker MP (1989) Visual responses in adult cat visual cortex depend on N-methyl-D-aspartate receptors. *Proc Natl Acad Sci USA* 86:5183–5187.
34. Fox K, Sato H, Daw N (1989) The location and function of NMDA receptors in cat and kitten visual cortex. *J Neurosci* 9:2443–2454.
35. Bair W, Cavanaugh JR, Movshon JA (2003) Time course and time-distance relationships for surround suppression in macaque V1 neurons. *J Neurosci* 23:7690–7701.
36. Li Z (1999) Visual segmentation by contextual influences via intra-cortical interactions in the primary visual cortex. *Network* 10:187–212.
37. Johnson RR, Burkhalter A (1996) Microcircuitry of forward and feedback connections within rat visual cortex. *J Comp Neurol* 368:383–398.
38. Wang XJ (2001) Synaptic reverberation underlying mnemonic persistent activity. *Trends Neurosci* 24:455–463.
39. Kharazia VN, Phend KD, Rustioni A, Weinberg RJ (1996) EM colocalization of AMPA and NMDA receptor subunits at synapses in rat cerebral cortex. *Neurosci Lett* 210: 37–40.
40. Petralia RS, Yokotani N, Wenthold RJ (1994) Light and electron microscope distribution of the NMDA receptor subunit NMDAR1 in the rat nervous system using a selective anti-peptide antibody. *J Neurosci* 14:667–696.
41. Rosier AM, Arckens L, Orban GA, Vandesande F (1993) Laminar distribution of NMDA receptors in cat and monkey visual cortex visualized by [3H]-MK-801 binding. *J Comp Neurol* 335:369–380.
42. Eickhoff SB, Rottschy C, Zilles K (2007) Laminar distribution and co-distribution of neurotransmitter receptors in early human visual cortex. *Brain Struct Funct* 212: 255–267.
43. Rivadulla C, Sharma J, Sur M (2001) Specific roles of NMDA and AMPA receptors in direction-selective and spatial phase-selective responses in visual cortex. *J Neurosci* 21: 1710–1719.
44. Larkum ME, Nevian T, Sandler M, Polsky A, Schiller J (2009) Synaptic integration in tuft dendrites of layer 5 pyramidal neurons: A new unifying principle. *Science* 325: 756–760.
45. Rockland KS, Virga A (1989) Terminal arbors of individual "feedback" axons projecting from area V2 to V1 in the macaque monkey: A study using immunohistochemistry of anterogradely transported Phaseolus vulgaris-leucoagglutinin. *J Comp Neurol* 285:54–72.
46. Herrero JL, et al. (2008) Acetylcholine contributes through muscarinic receptors to attentional modulation in V1. *Nature* 454:1110–1114.
47. Lamme VA, Zipser K, Spekreijse H (1998) Figure-ground activity in primary visual cortex is suppressed by anesthesia. *Proc Natl Acad Sci USA* 95:3263–3268.
48. Xing D, Yeh CI, Shapley RM (2009) Spatial spread of the local field potential and its laminar variation in visual cortex. *J Neurosci* 29:11540–11549.
49. Supèr H, Roelfsema PR (2005) Chronic multiunit recordings in behaving animals: Advantages and limitations. *Prog Brain Res* 147:263–282.